Mode-coupling theory for the glass transition: Test of the convolution approximation for short-range interactions

A. Ayadim, Ph. Germain, and S. Amokrane
Physique des Liquides et Milieux Complexes, Faculté des Sciences et Technologie, Université Paris-Est (Créteil), 61 Avenue du Général de Gaulle, FR-94010 Créteil Cedex, France
(Received 3 October 2011; published 5 December 2011)

We reexamine the convolution approximation commonly used in the mode-coupling theory (MCT) of nonergodic states of classical fluids. This approximation concerns the static correlation functions used as input in the MCT treatment of the dynamics. Besides the hard-sphere model, we consider interaction potentials that present a short-range tail, either attractive or repulsive, beyond the hard core. By using accurate static correlation functions obtained from the fundamental measures functional for hard spheres, we show that the role of three-body direct correlations can be more significant than what is inferred from previous simple ansatzs for pure hard spheres. This may in particular impact the location of the glass transition line and the nonergodicity parameter.

DOI: 10.1103/PhysRevE.84.061502 PACS number(s): 64.70.Q−, 82.70.Dd, 82.70.Gg

I. INTRODUCTION

Understanding the nonergodic states that are frequently observed in soft condensed matter, as for example, colloidal gels, motivated numerous experimental and theoretical studies for several decades now, first for their practical interest. On the other hand, the presence in soft matter of a new mechanism of dynamical arrest, the attractive glass [1], that differs from the "caging" responsible for the repulsive glass in molecular systems has given a new impetus to the study of the glassy states (see also [2–4] for reviews). The MCT analysis of dynamically arrested states in colloids extends to Brownian particles the concepts originally developed for molecular fluids [5]. This application of the MCT theoretical framework [6], originally elaborated for dense fluids [7,8], raises different questions. Some of them are relative to the assumptions made to obtain the MCT equations for the dynamics of the density fluctuations. For example, dynamical heterogeneities or cluster aggregation neglected in the MCT are expected to be relevant [1,4] in low density states, like gels. This is why more advanced versions of the mode-coupling theory have been developed [9–12], which aim at a more complete description of this dynamics. On the other hand, alternatives to the MCT have also been proposed [13,14]. Aside from these important questions, it is useful to examine further, in the framework of the MCT, the approximations made for the static input, in particular the convolution approximation. This is the main goal of this paper.

In the MCT, the dynamical arrest, or nonergodicity transition, is characterized by the nonvanishing of the long-time limit of the density autocorrelation function $\langle \rho(\mathbf{q},t\to\infty)\rho(-\mathbf{q},t=0)\rangle$, where $\rho(\mathbf{q},t)$ is the Fourier transform of the microscopic particle density. The MCT dynamic properties are entirely determined by the static correlation functions and involve the two-body and three-body direct correlation functions (dcfs) $c^{(2)}(\mathbf{q})$ and $c^{(3)}(\mathbf{q})$ (in Fourier space) through a vertex function from which the memory kernel is computed. While accurate methods have been developed for $c^{(2)}$ [15], much less is known about $c^{(3)}$. This question is eluded in the convolution approximation, which assumes $c^{(3)}(\mathbf{q})=0$. This approximation, not fundamental in the MCT, was substantiated by a work by Barrat *et al.* [16] on the hard-sphere (HS) fluid. The authors used for $c^{(2)}$ the analytical solution of the Percus-Yevick (PY) closure of the Ornstein-Zernike (OZ) equations [15] and for $c^{(3)}$ an expression proposed by Denton and Ashcroft [17] (DA) based on a combination of the PY two-body dcfs. Accordingly, they showed that within this class of trial functions, the density of the glass transition depends weakly on $c^{(3)}$: the critical packing fraction changes from 0.516 with $c^{(3)}=0$ to 0.512 with $c^{(3)}\neq 0$. The convolution approximation then became widely admitted, and generalized to various situations, including mixtures or non-HS interactions. It was discussed only for some specific mixtures by Sciortino *et al.* [18], who also showed that the incorporation of $c^{(3)}$ has little effect on the nonergodicity parameter for Lennard-Jones mixtures, but that it is important to include it for silica. Except for this case, the convolution approximation has systematically been used in the applications of the MCT. We shall examine here simple ways to improve it, on the basis of sufficiently accurate expressions of $c^{(3)}$, beyond the simple ansatzs, that exist for hard spheres (we will also use more accurate two-body dcfs $c^{(2)}$, known to be required for some interaction potentials [19,20]). The influence of the three-body HS contribution on two quantities will be examined: the critical packing fraction of the glass transition, and the long-time density correlation function which determines the Debye-Waller factor and some mechanical properties of the glass.

We study first the HS model for which these triplet correlations are fully incorporated. We next consider the addition of a short-range tail. In this case we also use the HS contribution to $c^{(3)}$, with a suitably defined hard-sphere diameter. The practical reason for this is the scarcity of accurate expressions for the non hard-sphere contribution (see, for example, [21,22] for soft spheres and the Lennard Jones fluid). On the other hand, simple geometric arguments suggest that the dominant contributions to $c^{(3)}$ should originate for hard-sphere-like particles mostly from the (effective) hard-core interaction. *A contrario*, a great sensitivity to details in $c^{(3)}$ would raise the very question of neglecting three-body contribution and the necessity of describing $c^{(3)}$ beyond the HS contribution.

This paper is hence organized as follows: Sec. II presents the theoretical methods, Sec. III presents the results, and Sec. IV presents the conclusion.

II. THEORY

A. Mode-coupling theory of dynamical arrest for colloidal particles

We briefly recall here the MCT treatment of the nonergodicity transition in colloids. The mode-coupling theory introduced by Kawasaki [23] was originally used for molecular glasses [6]. The central assumption is that the dynamics is dominated by collective modes. They reduce for colloids to the particles density [5]. By factorizing four-point correlations into a product of two-point terms (assumption of independent modes) one obtains a closed equation for the coherent intermediate scattering function $S(q;t)$:

$$S(q;t) = \frac{1}{N}\langle \rho(\mathbf{q},t)\rho(-\mathbf{q},0)\rangle \tag{1}$$

whose transform in the frequency domain is the dynamic structure factor $S(q;\omega)$. In the MCT for colloids, the time evolution of $S(q;t)$ without hydrodynamic interactions obeys the equation [24]

$$\frac{\partial}{\partial t}S(q;t) + q^2\frac{D_0}{S(q)}S(q;t) + \frac{1}{D_0}\int_0^t dt' M(q;t-t')\frac{\partial}{\partial t'}S(q;t') = 0, \tag{2}$$

where D_0 is the Stoke-Einstein diffusion coefficient and $M(\mathbf{q},t)$ is the memory kernel:

$$M(q,t) = \frac{\rho}{2}D_0^2\int\frac{d^3k}{(2\pi)^3}V^2(\mathbf{q},\mathbf{k})S(\mathbf{k};t)S(\mathbf{q}-\mathbf{k};t). \tag{3}$$

In this expression $V(\mathbf{q},\mathbf{k})$ is the vertex function

$$V(\mathbf{q},\mathbf{k}) = \frac{1}{q}[\mathbf{q}\cdot(\mathbf{q}-\mathbf{k})c^{(2)}(\mathbf{q}-\mathbf{k}) + \mathbf{q}\cdot\mathbf{k}\,c^2(k) + \rho q^2 c^{(3)}(\mathbf{k},\mathbf{q}-\mathbf{k})] \tag{4}$$

with ρ as the number density (for hard spheres of diameter σ, the packing fraction is $\eta = \frac{\pi}{6}\rho\sigma^3$). The actual wave vectors as they appear in the $c^{(3)}$ term [24] are consistent with the derivation in Ref. [5] but they differ from those in Ref. [18]. In these equations, the static structure factor $S(q) = [1-\rho c^{(2)}(q)]^{-1}$ is related to $c^{(2)}$ by the OZ equation (in q space). Equations (2)–(4) govern the time evolution of $S(q;t)$. Since we are interested here in a simple illustration of the impact of $c^{(3)}$, we will consider only its long-time limit. $S(q,t\to\infty)$ can be determined without solving Eq. (2) at all times, which is numerically more demanding. In an ergodic fluid, $S(q,t\to\infty) = 0$. The ideal glass is defined by $S(q,t\to\infty) \neq 0$. This arrested state is usually characterized by the nonergodicity parameter $f(q)$ (or glass form factor) defined by

$$S(q,t\to\infty) = S(q)f(q). \tag{5}$$

From the long-time limit of Eqs. (2)–(4), one gets the following equation for $f(q)$:

$$f(q) = \frac{m(q)}{1+m(q)} \tag{6}$$

with

$$m(\mathbf{q}) = \frac{1}{2}\int\frac{d^3k}{(2\pi)^3}\tilde{V}(\mathbf{q},\mathbf{k})f(\mathbf{k})f(\mathbf{q}-\mathbf{k}) \tag{7}$$

and

$$\tilde{V}(\mathbf{q},\mathbf{k}) = \frac{\rho}{q^2}V^2(\mathbf{q},\mathbf{k})S(q)S(k)S(\|\mathbf{q}-\mathbf{k}\|). \tag{8}$$

The physical solution of Eqs. (6) and (7) is the greatest one, in the range $0 \leqslant f(q) \leqslant 1$ [6]. It is the limit of the iteration process: $f^{(0)} = 1$, $f^{(n+1)} = \frac{F(f^{(n)})}{1+F(f^{(n)})}$, where the functional F is the right-hand side of Eq. (7). In the glass, $f(q)$ gives direct access to the Debye-Waller factor and to the longitudinal stress modulus $m_0 = m(q=0)$. From Eq. (7) this limit is

$$m_0 = \int_0^\infty W(k)f^2(k)dk \tag{9}$$

with

$$W(k) = \rho S_0\left[\frac{kS(k)}{2\pi}\right]^2\left\{[c^{(2)}(k)+\rho c^{(3)}(\mathbf{k},-\mathbf{k})]^2 + \frac{2}{3}k[c^{(2)}(k)+\rho c^{(3)}(\mathbf{k},-\mathbf{k})]\frac{dc^{(2)}(k)}{dk} + \frac{1}{5}\left[k\frac{dc^{(2)}(k)}{dk}\right]^2\right\}. \tag{10}$$

The function $W(k)$ follows from the limit $\mathbf{q}\to\mathbf{0}$ of Eqs. (7) and (8) with a proper account of the q^2 terms in the square of $V(\mathbf{q},\mathbf{k})$ given in Eq. (4) ($S_0 = \rho k_B T\chi^T$ is the static structure factor at zero wave number with χ^T the static susceptibility). Note that given the exact sum rule

$$\frac{\partial}{\partial\rho}c^{(2)}(k) = c^{(3)}(\mathbf{k},-\mathbf{k}), \tag{11}$$

$W(k)$ is determined solely by $c^{(2)}(k)$ and its density derivative. The effect on m_0 of different approximations of $c^{(3)}$ that obey Eq. (11) is then through $f(k)$. The importance of m_0 is shown, for example, by the sound velocity in the glass state: in the generalized hydrodynamic description [25] one finds at low frequency [26] $\hat{v}_0 = v_0\sqrt{1+m_0}$ with $v_0 = v/\sqrt{S_0}$ and $v = \sqrt{k_BT/m}$ the hydrodynamic and thermal velocities, respectively.[1]

To test the convolution approximation, we summarize in the next section the methods we used to compute $c^{(3)}$ for hard spheres beyond the simple ansatzs.

B. Three-body direct correlation function for hard spheres

In the density functional theory (DFT), the n-body dcf is given by the functional derivative

$$c^{(n)}(\mathbf{r}_1,\ldots,\mathbf{r}_n) = -\frac{\delta^{(n)}\beta F^{\mathrm{ex}}[\rho]}{\delta\rho(\mathbf{r}_1)\cdots\delta\rho(\mathbf{r}_n)}, \tag{12}$$

where $F^{\mathrm{ex}}[\rho]$ is the excess (over the ideal gas) free-energy functional. In Rosenfeld's fundamental measures functional

[1] In Ref. [25] the relation was written using the high frequency velocity v_∞ instead, replacing χ^T by that of the glass $\chi_q = \chi^T/(1+m_0)$, a result quoted in [27].

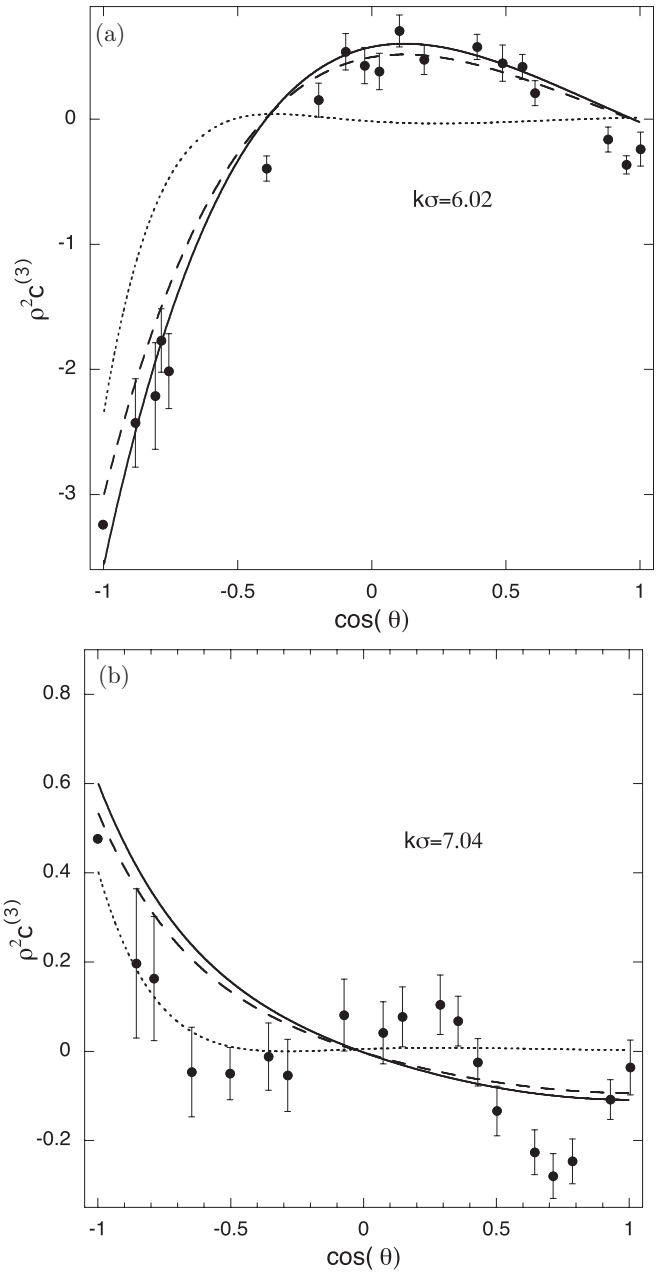

FIG. 1. Three-body direct correlation function for hard spheres from the density functional theory and the Denton-Aschcroft ansatz. The curves show $\rho^2 c^{(3)}(k, \cos\theta)$, with θ the angle $(\vec{q},\vec{k})$ in the isocele triangle geometry. Symbols: simulation [29]; solid line: Rosenfeld's FMF [28]; dashed line: modified FMF [32,33]; dotted line: DA anstaz. The packing fraction is $\eta = 0.45$.

(FMF) for hard spheres [28], it is taken as

$$F^{\rm ex} = k_B T \int d\mathbf{x}\Phi(\{n_\alpha(\mathbf{x})\}). \tag{13}$$

In its original form [28] the free-energy density Φ corresponds to the PY compressibility equation. It is a function of the weighted densities $n_\alpha(\mathbf{x}) = \int d\mathbf{x}'\rho(\mathbf{x}')w_\alpha(\mathbf{x}-\mathbf{x}')$ obtained from the actual density $\rho(x)$ through convolution with weights w_α. The FMF uses four scalar and two vectorial weights (see the Appendix for details). In Fourier space one obtains from

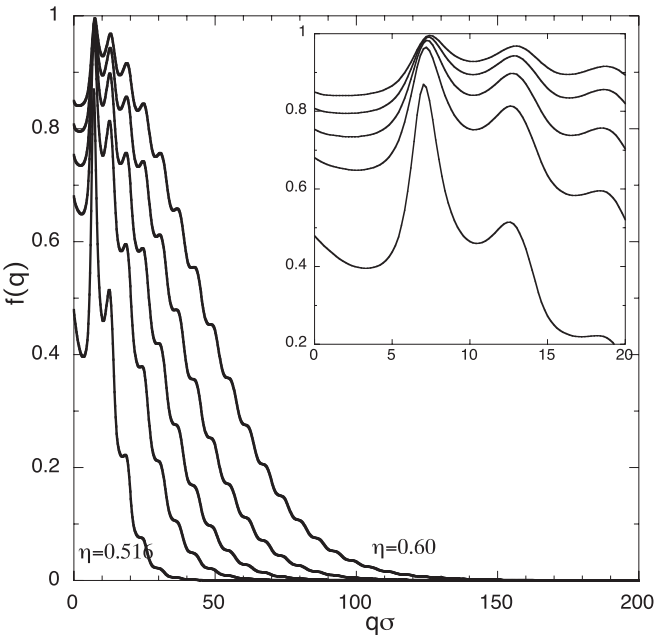

FIG. 2. $f(q)$ with $c^{(2)}_{\rm PY}$ and $c^{(3)} = 0$. From left to right: $\eta = 0.516$, 0.54, 0.56, 0.58, and 0.60. Inset: small q region.

Eqs. (12) and (13)

$$c^{(3)}_{ijk}(\mathbf{q}_1,\mathbf{q}_2,\mathbf{q}_3) = -\sum_{\alpha,\beta,\gamma} \frac{\partial^{(3)}\Phi}{\partial n_\alpha \partial n_\beta \partial n_\gamma} w_i^\alpha(\mathbf{q}_1) w_j^\beta(\mathbf{q}_2) w_k^\gamma(\mathbf{q}_3) \times \delta_{\mathbf{q}_3,-\mathbf{q}_1-\mathbf{q}_2}. \tag{14}$$

This expression is given here for the general case of a mixture (the Appendix of Ref. [29] lists the 32 contributions). We have checked that when the vectorial terms are computed with the correct sign, using the original FMF or that of Kierlik

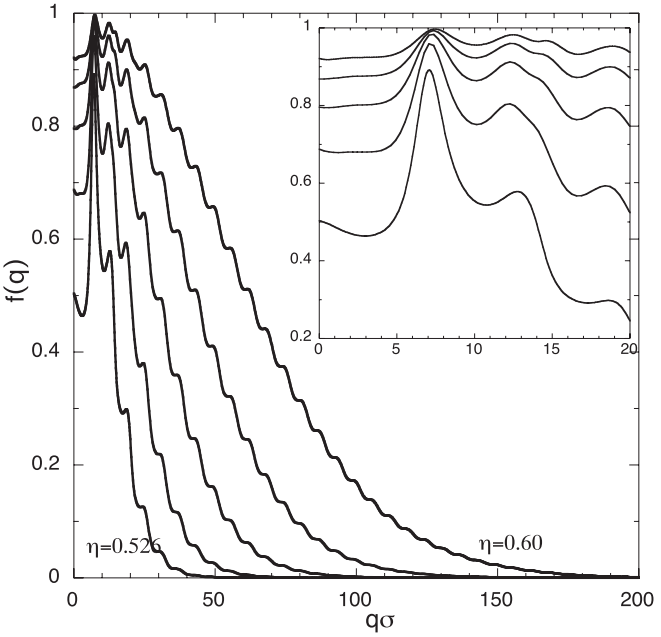

FIG. 3. $f(q)$ with $c^{(2)}_{\rm RHNC}$ using the Labik-Malijevski bridge function [37] and $c^{(3)} = 0$. From left to right: $\eta = 0.526$, 0.54, 0.56, 0.58, and 0.60.

and Rosinberg [30,31] with purely scalar weights, gives the same $c^{(3)}$. An example is shown in Fig. 1, which also shows the results obtained with Φ^{CS} [32,33] corresponding to the Boublik, Mansoori, Carnahan, Starling, and Leland (BMCSL) equation of state [34], and those with the DA ansatz. Note that there exists an alternative route to $c^{(3)}$ based on the inhomogeneous integral equations theory (see, for example, [35]) but its implementation is more involved than that of Eq. (14).

III. RESULTS

A. Hard-sphere fluid

1. Influence of the closure for $c^{(2)}$ in the convolution approximation

To better separate the influence of different static input, we first reexamine the sensitivity to $c^{(2)}$, when $c^{(3)} = 0$. To this end, the critical packing fraction η_c of the glass transition was determined by using the PY and the reference hypernetted chain (RHNC) closures [36] with the bridge function of Labik and Malijevsky [37]. We found $\eta_c^{PY} = 0.516$ as in [16], and $\eta_c^{\mathrm{RHNC}} = 0.526$. η_c is thus not very sensitive to the closure of the OZ equation. The nonergodicity parameter $f(q)$ was next computed for packing fractions above η_c. Figures 2 and 3 show the behavior of $f^{\mathrm{PY}}(q)$ and $f^{\mathrm{RHNC}}(q)$ for $\eta_c \leqslant \eta \leqslant 0.60$. Both show similar trends: broadening of $f(q)$ and simultaneous increase of $f(0)$ when η increases. This indicates a stronger localization of the caged particles and long-range correlations of the density fluctuations, as expected. Besides these similarities, quantitative differences are however observed at high density (Fig. 4). $f(q)$ extends over a greater range with the RHNC input than with the PY one: For $\eta = 0.60$, a simple Gaussian approximation $f(q) \approx \exp(-q^2 r_{\mathrm{loc}}^2/6)$ [38] gives a localization length $r_{\mathrm{loc}}^{\mathrm{RHNC}} \approx 0.033\sigma$ instead of $r_{\mathrm{loc}}^{\mathrm{PY}} \approx 0.045\sigma$.

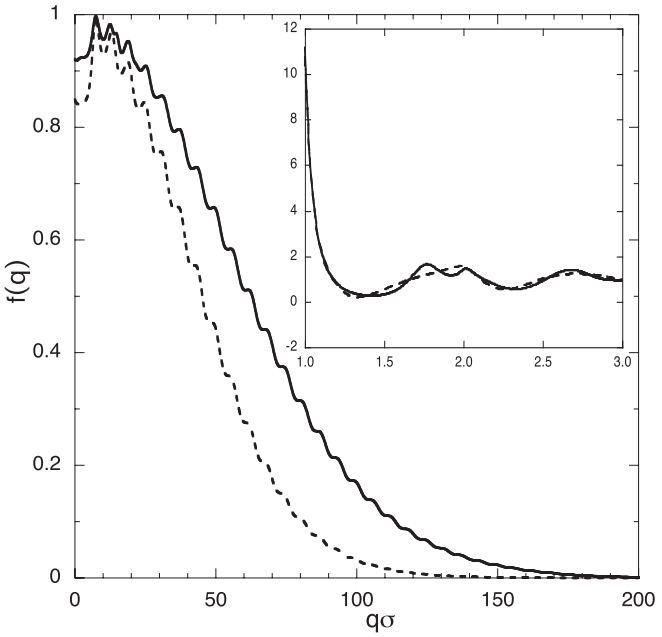

FIG. 4. Influence of the closure for $c^{(2)}$ on $f(q)$ for $c^{(3)} = 0$: solid line: RHNC; dashed line: PY. Inset: radial distribution function $g(r)$. The packing fraction is $\eta = 0.6$.

Additionally, the long wavelength value $f_0 = f(q = 0)$ is greater for RHNC than for PY. This leads to a significant difference for the longitudinal stress modulus: $m_0^{\mathrm{RHNC}} = 11.7$ instead of $m_0^{\mathrm{PY}} = 5.62$, a result of the strong variation of $m_0 = \frac{f_0}{1-f_0}$ for $f_0 \approx 1$. Thus, in spite of qualitative similarities, the insufficiency of the PY static input for describing some dynamical properties of the glass at high density is evidenced at the two-body level. This is already known for the static properties, in particular the pair distribution function, which exhibits at high density a double peak not shown by $g^{\mathrm{PY}}(r)$ (see inset in Fig. 4). The structural origin of this split second peak (see, e.g., [39]) is still debated (see, for example, [40]). Concerning the nonergodicity transition, the necessity of accurate static input was already shown in the case of low density gels of HS with short-ranged attractive interactions [20,41]. This is confirmed here also for pure HS fluids, independently of the question of the convolution approximation.

2. Influence of $c^{(3)}$

We summarize here the results for η_c and $f(q)$, for two versions of $c^{(3)}$: the Denton-Ashcroft ansatz ($c_{\mathrm{DA}}^{(3)}$) constructed with $c_{\mathrm{PY}}^{(2)}$, and $c^{(3)}$ from Rosenfeld's FMF ($c_{\mathrm{Ros}}^{(3)}$), that is, with the free energy density Φ^{PY} (using Φ^{CS} gives essentially the same results). When comparing both versions of $c^{(3)}$, we used for consistency $c_{\mathrm{PY}}^{(2)}$ (the functional used to compute $c_{\mathrm{Ros}}^{(3)}$ is also consistent with $c_{\mathrm{PY}}^{(2)}$). We will designate this combination $c_{\mathrm{PY}}^{(2)}/c_{\mathrm{Ros}}^{(3)}$ as the PY approximation. However, as $c_{\mathrm{RHNC}}^{(2)}$ is more accurate at high density, we also used the combination $c_{\mathrm{RHNC}}^{(2)}/c_{\mathrm{Ros}}^{(3)}$, referred to as the RHNC approximation. Both approximations for $c^{(3)}$ lead to similar trends for the nonergodicity transition. With $c_{\mathrm{PY}}^{(2)}$ we found critical packing fractions $\eta_c^{\mathrm{DA}} = 0.516$ and $\eta_c^{\mathrm{Ros}} = 0.504$. The value of η_c^{DA} is the same as in the convolution approximation. With $c_{\mathrm{RHNC}}^{(2)}$ we observe a similar impact of $c_{\mathrm{Ros}}^{(3)}$: $\eta_c^{\mathrm{Ros}} = 0.509$, instead of $\eta_c = 0.526$ for $c^{(3)} = 0$ (these values are probably the correct MCT ones with the appropriate static input). The effect of $c_{\mathrm{Ros}}^{(3)}$ on the critical packing fraction is thus greater than with the DA ansatz, although it remains moderate. Recalling the simulation value $\eta_c^{\mathrm{MD}} = 0.58$, we observe that incorporating static triplet correlations worsens the MCT prediction for the extension of the domain of glassy states.

For a given $c^{(2)}$, the behavior of $f(q)$ with η is qualitatively similar for all versions of $c^{(3)}$, viz the one observed for $c^{(3)} = 0$: broadening of $f(q)$ and increase of the long wavelength value f_0 when η increases beyond η_c. The effect of $c^{(3)}$ with $c_{\mathrm{PY}}^{(2)}$ is shown in Fig. 5 for $\eta = 0.52$: while it is hardly observable with $c_{\mathrm{DA}}^{(3)}$, it is more significant with $c_{\mathrm{Ros}}^{(3)}$, as for the value of η_c. The inset shows the same effect of $c_{\mathrm{Ros}}^{(3)}$ with $c_{\mathrm{RHNC}}^{(2)}$. For $q = 0$, one gets in this case $m_0 = 1.98$ for $c_{\mathrm{Ros}}^{(3)}$ instead of $m_0 = 1.50$ with $c^{(3)} = 0$ (the localization length r_{loc} is the same as in the convolution approximation). For $\eta = 0.6$, this effect of $c^{(3)}$ is less important. This is coherent with the idea that the caging effect should be determined mostly by the hard-core repulsion between pairs when approaching the random close packing.

Finally, we can also conclude here about the choice for the static input in the MCT for hard spheres: the most accurate

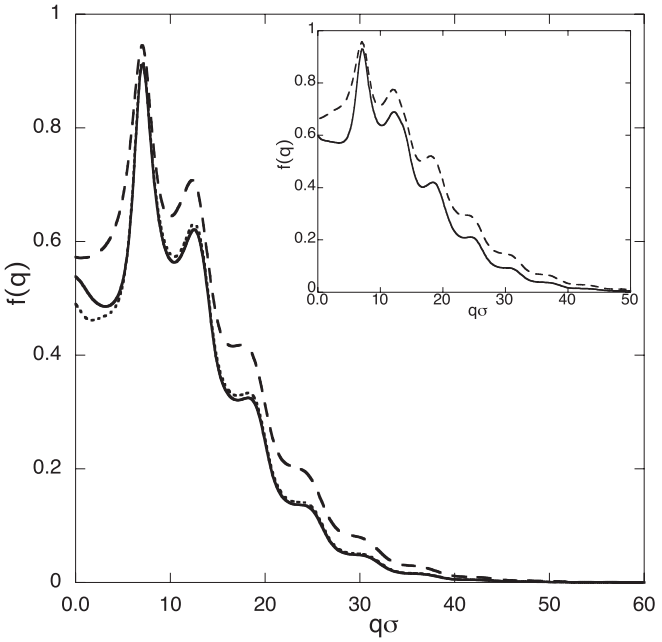

FIG. 5. Influence of $c^{(3)}$ on $f(q)$ with $c^{(2)}_{\rm PY}$. Solid line: $c^{(3)}=0$; dashed line: $c^{(3)}_{\rm Ros}$; dotted line: $c^{(3)}_{\rm DA}$ for $\eta=0.52$. Inset: same with $c^{(2)}_{\rm RHNC}$ and $\eta=0.53$.

description is the one that combines the RHNC closure for $c^{(2)}$ and the $c^{(3)}$ from DFT, presently with Rosenfeld's FMF. In trying to understand this from the q dependence of the correlation functions, we found a more complex scenario than for the other versions of $c^{(3)}(q)$. The latter have little influence for $q\approx q_0$, the position of the main peak of $S(q)$, that gives indeed the leading contribution to the memory kernel $m(q)$ [see Eqs. (4) and (7)]. With $c^{(3)}_{\rm Ros}$ the small-q part in the vertex function is more important. This explains the increase observed in m_0.

B. Short-range hard-core Yukawa potential

We now consider the addition of a short-range Yukawa tail to the HS potential: $\beta V(r)=\frac{1}{T^*}\exp[-\kappa(\frac{r}{\sigma}-1)]/r$, where $T^*=k_BT/\epsilon$ and κ are the reduced temperature and inverse range, respectively. The case of attractions ($\epsilon<0$) has been extensively studied, because it may lead for very short ranges to attractive glasses, or low density gelation [1,2,4,19]. For such potentials, besides the question of the dynamic heterogeneity [1,4,42], the consequences of the convolution approximation on the MCT predictions has not yet been checked. We thus computed the MCT glass transition line for an attractive Yukawa potential as follows: for the two-body dcf we used $c^{(2)}_{\rm RHNC}$ since an accurate $c^{(2)}$ is required for short-range attractions [19,20] (here with $\kappa=20$). For the three-body contribution now, we incorporated only the HS contribution through $c^{(3)}_{\rm Ros}$. This amounts to considering that the effect of a third particle on a pair of neighboring particles (that form "bonds" in attractive glasses) is mainly to reduce the volume accessible to the pair, due to the exclusion sphere of the third particle. This should be an acceptable approximation for very short attraction ranges, as in this case the excluded volume exceeds that of the attraction shell (Fig. 6). The latter, having the radius of the exclusion sphere and a thickness of the order

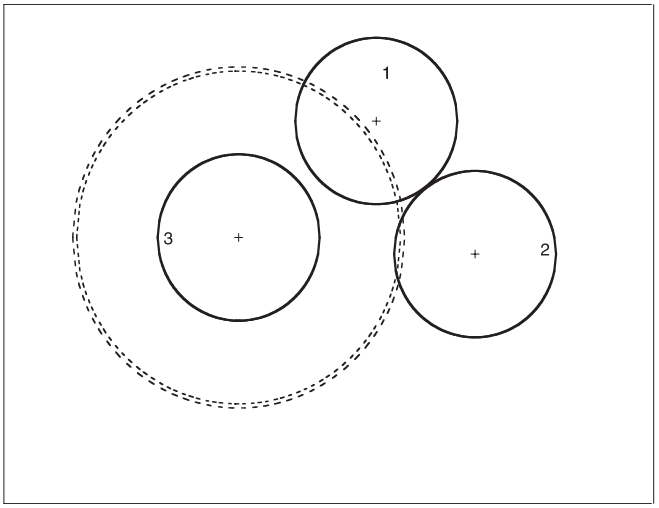

FIG. 6. Triplet configuration showing a particle (filled circle labeled 3) approaching a bonded pair (1 and 2). The short dashes show the exclusion sphere of particle (3) for the pair. These particles (1) (2) experience an attractive interaction with (3) when their centers lie in the shell between the short and the long dashes and whose thickness is the attraction range.

of the range of the tail, corresponds to distances between the centers of the spheres for which the potential is attractive. In this case, the effective diameter used in $c^{(3)}_{\rm Ros}$ is simply the actual HS diameter σ. The results are shown in Fig. 7. We also computed the MCT glass line using the DA ansatz for $c^{(3)}$ (still with the HS contribution): the transition line and the nonergodicity factors do not depart much from those for $c^{(3)}=0$. The effect $c^{(3)}_{\rm Ros}$ is however more significant, since it extends the domain of the attractive glass to higher temperatures. For analyzing the underlying mechanism, we compute $r_{\rm loc}$ in the Vineyard approximation for $T^*=0.3$ since the onset of gelation occurs close to this temperature

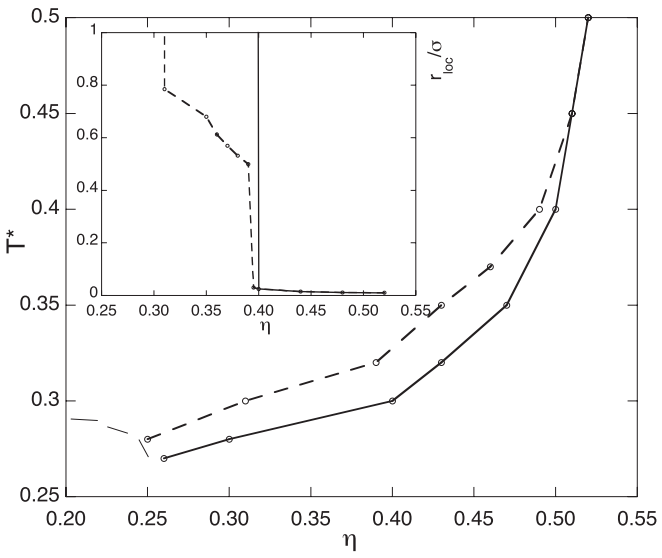

FIG. 7. Nonergodicity line for the attractive Yukawa fluid. Solid line: $c^{(2)}_{\rm RHNC}$ and $c^{(3)}=0$; dashed line: $c^{(2)}_{\rm RHNC}$ and $c^{(3)}_{\rm Ros}$ (the long dashes show the RHNC nonconvergence domain). Inset: same for the localization length.

for $\kappa = 20$. The transition packing fractions are $\eta_c = 0.40$ for $c^{(3)} = 0$ and $\eta_c = 0.31$ with $c^{(3)}_{\rm Ros}$. For $c^{(3)} = 0$, the particles are strongly localized for $\eta \approx 0.40$ ($r_{\rm loc} = 0.025$), as expected from the picture of long-lived bonds induced by the short-range attraction, while they are diffusive for $\eta < 0.40$ in the ergodic liquid ($r_{\rm loc} \to \infty$). The incorporation of the HS contribution $c^{(3)}_{\rm Ros}$ leads to an intermediate situation for $0.31 < \eta < 0.40$: in this state $r_{\rm loc}$ is still finite, but its value is much greater (it is also greater than for an ordinary repulsive glass). One can understand that in the density (or temperature) range in which the bonding mechanism is insufficient for stabilizing the arrested state, the diffusion of the particles is limited by the HS three-body correlations. The value of $r_{\rm loc}$ might then be related to the typical size of the structure formed by the network of particles in the gel. Nevertheless, one should be reminded that only the HS contribution to the triplet correlations is considered here, so that the picture might be more complex with the complete $c^{(3)}$. This clearly raises the question of its accurate description beyond the situation of pure HS interactions. As already stressed in previous work, this is important for an accurate determination of the static input even for a simple LJ fluid [22] or for accounting for many-body effects in the effective fluid representation of size asymmetric mixtures [43].

We also considered the case of a repulsive Yukawa tail ($\epsilon > 0$). As for the attractive one, $c^{(3)}$ was calculated using Rosenfeld's functional for hard spheres. To begin with, the repulsive tail was completely neglected, $c^{(3)}_{\rm Ros}$ being computed using the actual hard-core diameter σ. To go beyond this, however, the simplest idea consists in defining an effective HS diameter, as, for example, in the Barker-Henderson perturbative treatment [15] of soft potentials:

$$\sigma^{\rm eff} = \int_0^\infty dr\{1 - \exp[-\beta V(r)]\}. \qquad (15)$$

This approximation, accounting grossly for the effect of the additional soft repulsion ($\sigma^{\rm eff} > \sigma$ here), usually gives acceptable results for the equilibrium quantities (the free energy for instance). However, its consequences for the glass transition are unknown. We then anticipate that the softer the interaction, the larger the overestimation of the caging effect in the dense fluid. We thus took a rather steep repulsive tail, with $\kappa = 10$. We show in Fig. 8 the nonergodicity factor $f(q)$ in the glassy state for $T^* = 1$ and $\eta = 0.52$, computed with $c^{(3)} = 0$ and $c^{(3)} = c^{(3)}_{\rm Ros}$ using either the true hard-core diameter σ or the effective one $\sigma^{\rm eff}$ from Eq. (15). In both cases, $f(q)$ is enhanced by $c^{(3)}$, but the effect is much greater with the latter [in the former one the increase of $f(q)$ is comparable to what was observed with the previous potentials]. It is particularly strong for $q \leqslant q_0$. As replacing the Yukawa tail by a purely HS interaction probably exaggerates the caging effect, one would expect the actual $f(q)$ to be between these two curves. We observed similar features on the MCT transition line (not shown here), which is markedly moved toward lower densities since $\sigma^{\rm eff} > \sigma$ (recall that η grows as the cube of the HS diameter). This raises again the need of an accurate description of $c^{(3)}$ beyond the hard-sphere model for assessing the present estimates for repulsive tails.

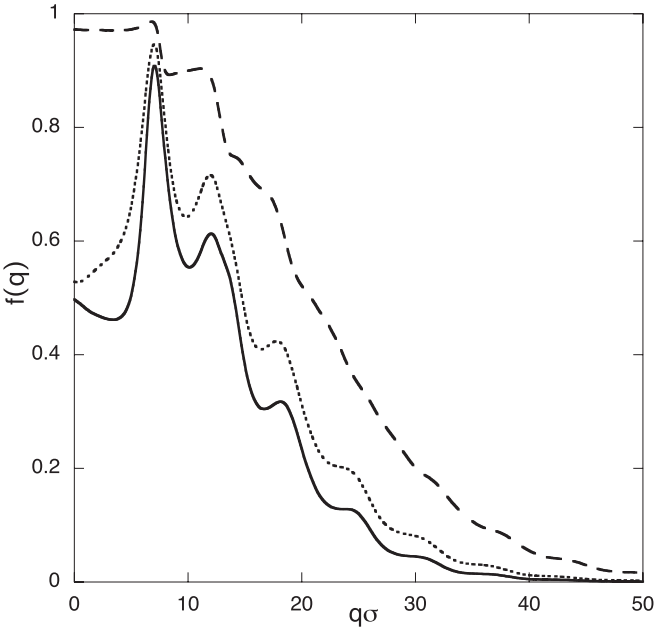

FIG. 8. Influence on $f(q)$ of the effective HS diameter used in $c^{(3)}_{\rm Ros}$ for the repulsive Yukawa at $\eta = 0.52$. Solid line: $c^{(3)} = 0$; dotted line: $\sigma^{\rm eff} = \sigma$; dashed line: $\sigma^{\rm eff} > 1.073\sigma$ from Eq. (15).

IV. CONCLUSION

In this paper we discussed the effect of the three-body direct correlations function $c^{(3)}$ on some properties of the dynamically arrested states as described by the mode-coupling theory. In particular, we studied its effect on the packing fraction of the ideal glass transition and the nonergodicity factor. This was done for the pure hard-sphere fluid and for interaction potentials between the particles having in addition a short-range tail, either attractive or repulsive. This was motivated by the fact that while the basic approximations of the MCT have been discussed in several theoretical works, even recently [1,4,44], the convolution approximation concerning the static input which assumes $c^{(3)} = 0$ is generally readily accepted. More precisely, a sizable effect of the triplet correlations on the nonergodicity factor has already been found for specific mixtures [18], but this question is generally eluded without further discussion. It was actually known that, in certain circumstances, a fine description of the static input, already at the two-body level, can be important for an accurate determination of the glass transition line [19,20]. While confirming that the effect of $c^{(3)}$ is indeed negligible when using the early ansatz proposed in [17], we have shown that using $c^{(3)}$ from an accurate density functional theory may have a more significant effect. For the hard-sphere fluid, the glass transition packing fraction is slightly decreased with respect to that obtained in the convolution approximation. The second effect for hard spheres is to increase the nonergodicity factor, in particular at small q, which thus modifies the Debye-Waller factor and the longitudinal stress modulus m_0. For the attractive hard-core Yukawa fluid, the HS contribution to the triplet correlations enhances the stability of the attractive bonds with an ensuing extension of the attractive glass domain to higher temperatures. For the repulsive hard-core Yukawa fluid, the strong sensitivity of the results to the choice of the

effective hard-sphere diameter functions raises the question of the appropriate treatment of the triplet correlations for soft repulsive interactions.

These observations suggest that the search of improved methods for computing $c^{(3)}$ beyond the hard-spheres term is worthwhile. They nevertheless show that in the various situations investigated, three-body direct correlations systematically reinforce the stability of the dynamically arrested state. This underlines one natural insufficiency of the mode-coupling theory, which is the overestimation of the dynamical arrest, due to the neglect of heterogeneities. It should also be interesting to analyze the relation of these results with the question raised concerning the determination of the dynamical properties solely from the two-body correlations [44]. It might well be that higher order correlations are more important for the dynamics than for the static properties.

APPENDIX

We summarize here the main quantities required in the modified fundamental measures functional given in Refs. [32,33]. The free-energy density $\Phi(\{n_\alpha\})$ consistent with the BMCSL equation [34] (superscript CS) contains scalar and vector contributions:

$$\Phi^{\mathrm{CS}}(\{n_\alpha(\mathbf{r})\}) = \Phi^{\mathrm{S(CS)}}(\{n_\alpha(\mathbf{r})\}) + \Phi^{\mathrm{V(CS)}}(\{n_\alpha(\mathbf{r})\}), \tag{A1}$$

$$\Phi^{\mathrm{S(CS)}} = -n_0 \ln(1-n_3) + \frac{n_1 n_2}{1-n_3} + \frac{1}{36\pi} \times \left[\frac{1}{n_3^2}\ln(1-n_3) + \frac{1}{n_3(1-n_3)^2}\right] n_2^3, \tag{A2}$$

$$\Phi^{\mathrm{V(CS)}} = -\frac{\mathbf{n}_{\mathrm{V1}}\cdot\mathbf{n}_{\mathrm{V2}}}{1-n_3} - \frac{1}{12\pi}\left[\frac{1}{n_3^2}\ln(1-n_3) + \frac{1}{n_3(1-n_3)^2}\right] \times n_2 \mathbf{n}_{\mathrm{V2}}\cdot\mathbf{n}_{\mathrm{V2}}. \tag{A3}$$

The weighted densities are computed in Fourier space as $\tilde{n}_\alpha(\mathbf{k}) = \sum_i \rho_i(\mathbf{k})\tilde{\omega}_i^{(\alpha)}(-\mathbf{k})$, where the Fourier transforms of the weight functions $\tilde{\omega}_i^{(\alpha)}$ are

$$\begin{aligned} \frac{\tilde{\omega}_i^{(q)}(k)}{R_i^{(q)}} &= \frac{\sin(kR_i)}{kR_i}, \quad q = 0,1,2, \\ \frac{\tilde{\omega}_i^{(3)}(k)}{R_i^{(3)}} &= 3\frac{\sin(kR_i) - kR_i\cos(kR_i)}{(kR_i)^3}, \\ \tilde{\omega}_i^{(\mathrm{V2})}(\mathbf{k}) &= (-1)^{\frac{1}{2}}\mathbf{k}\tilde{\omega}_i^{(3)}(k), \quad \tilde{\omega}_i^{(\mathrm{V1})}(\mathbf{k}) = \frac{\tilde{\omega}_i^{(\mathrm{V2})}(\mathbf{k})}{4\pi R_i} \end{aligned} \tag{A4}$$

with $R_i^{(q)} = 1, R_i, S_i, V_i$ for $q = 0, 1, 2, 3$, respectively (R_i, S_i, V_i denote the hard-sphere radius, the surface area, and the volume of the sphere of species i).

[1] J. Bergenholtz and M. Fuchs, Phys. Rev. E **59**, 5706 (1999); J. Phys. Condens. Matter **11**, 10171 (1999).
[2] K. Dawson, Curr. Opin. Colloid Interface Sci. **7**, 218 (2002).
[3] F. Sciortino and P. Tartaglia, Adv. Phys. **54**, 471 (2005).
[4] E. Zaccarelli, J. Phys. Condens. Matter **19**, 323101 (2007).
[5] G. Szamel and H. Löwen, Phys. Rev. A **44**, 8215 (1991).
[6] W. Götze, in *Liquids, Freezing and Glass Transition*, edited by J.-P. Hansen, D. Levesque, and J. Zinn-Justin (North-Holland, Amsterdam, 1991), p. 287.
[7] U. Bengtzelius, W. Götze, and A. Sjolander, J. Phys. C **17**, 5915 (1984).
[8] W. van Megen and S. M. Underwood, Phys. Rev. E **49**, 4206 (1994).
[9] K. Kroy, M. E. Cates, and W. C. K. Poon, Phys. Rev. Lett. **92**, 148302 (2004).
[10] J. Wu and J. Cao, Phys. Rev. Lett. **95**, 078301 (2005).
[11] G. Biroli, J. P. Bouchaud, K. Miyazaki, and D. R. Reichman, Phys. Rev. Lett. **97**, 195701 (2006).
[12] G. Szamel and E. Flenner, Phys. Rev. E **81**, 031507 (2010).
[13] G. Szamel, Phys. Rev. Lett. **90**, 228301 (2003).
[14] M. A. Chávez-Rojo and M. Medina-Noyola, Phys. Rev. E **72**, 031107 (2005); **76**, 039902(E) (2007); R. Juárez-Maldonado and M. Medina-Noyola, Phys. Rev. Lett. **101**, 267801 (2008); M. A. Chávez-Rojo and M. Medina-Noyola, Phys. Rev. E **77**, 051503 (2008).
[15] J. P. Hansen and I. R. McDonald, *Theory of Simple Liquids* (Academic, London, 2005).
[16] J. L. Barrat, W. Götze, and A. Latz, J. Phys. Condens. Matter **1**, 7163 (1989).
[17] A. R. Denton and N. W. Ashcroft, Phys. Rev. A **39**, 426 (1989).
[18] F. Sciortino and W. Kob, Phys. Rev. Lett. **86**, 648 (2001); W. Kob, M. Nauroth, and F. Sciortino, J. Non-Crystal. Sol. **307**, 181 (2002).
[19] G. Foffi, G. D. McCullagh, A. Lawlor, E. Zaccarelli, K. A. Dawson, F. Sciortino, P. Tartaglia, D. Pini, and G. Stell, Phys. Rev. E **65**, 031407 (2002).
[20] Ph. Germain and S. Amokrane, Phys. Rev. E **76**, 031401 (2007).
[21] J. L. Barrat, J. P. Hansen, and G. Pastore, Mol. Phys. **63**, 747 (1988).
[22] S. Amokrane and J. G. Malherbe, Mol. Phys. **101**, 495 (2003).
[23] K. Kawasaki, Ann. Phys. (NY) **61**, 1 (1970).
[24] G. Nägele, J. Bergenholtz, and J. K. G. Dhont, J. Chem. Phys. **110**, 7037 (1999).
[25] W. Götze and M. R. Mayr, Phys. Rev. E **61**, 587 (2000).
[26] S.-H. Chong, Phys. Rev E **74**, 031205 (2006).
[27] E. Zaccarelli, G. Foffi, K. A. Dawson, F. Sciortino, and P. Tartaglia, Phys. Rev. E **63**, 031501 (2001).
[28] Y. Rosenfeld, J. Chem Phys. **98**, 8126 (1993).
[29] Y. Rosenfeld, D. Levesque, and J. J. Weis, J. Chem. Phys. **92**, 6818 (1990).
[30] E. Kierlik and M. L. Rosinberg, Phys. Rev. A **42**, 3382 (1990).
[31] S. Phan, E. Kierlik, M. L. Rosinberg, B. Bildstein, and G. Kahl, Phys. Rev. E **48**, 618 (1993).
[32] R. Roth, R. Evans, A. Lang, and G. Kahl, J. Phys. Condens. Matter **14**, 12063 (2002).
[33] Y. Yu and J. Wu, J. Chem. Phys. **117**, 10156 (2002).
[34] T. Boublik, J. Chem. Phys. **53**, 471 (1970); G. A. Mansoori, N. F. Carnahan, K. E. Starling, and T. W. Leland Jr., *ibid.* **54**, 1523 (1971).

[35] S. Jorge, E. Lomba, and J. Abascal, J. Chem. Phys. **116**, 730 (2002).
[36] F. Lado, S. M. Foiles, and N. W. Ashcroft, Phys. Rev. A **28**, 2374 (1983); F. Lado, Phys. Lett. **89**, 196 (1982).
[37] A. Malijevski and S. Labik, Mol. Phys. **60**, 663 (1987); S. Labik and A. Malijevski, *ibid.* **67**, 431 (1989).
[38] A. M. Puertas, M. Fuchs, and M. E. Cates, Phys. Rev. Lett. **88**, 098301 (2002); Phys. Rev. E **67**, 031406 (2003).
[39] J. Tobochnik and P. M. Chapin, J. Chem. Phys. **88**, 5824 (1988).
[40] B. O'Malley and I. Snook, J. Chem. Phys. **123**, 054511 (2005).
[41] Ph. Germain and S. Amokrane, Phys. Rev. E **81**, 011407 (2010).
[42] K. Schweizer, Curr. Opin. Colloid Interface Sci. **12**, 297 (2007).
[43] S. Amokrane, A. Ayadim, and J.-G. Malherbe, J. Phys. Condens. Matter **15**, 3443 (2003).
[44] L. Berthier and G. Tarjus, Phys. Rev. E **82**, 031502 (2010); L. Berthier and G. Biroli, Rev. Mod. Phys. **83**, 587 (2011).